

## Machine learning elucidates the anatomy of buried carbonate reef from seismic reflection data



Priyadarshi Chinmoy Kumar<sup>a,b</sup>, Kalachand Sain<sup>a,b,\*</sup>

<sup>a</sup> Wadia Institute of Himalayan Geology, 33 GMS Road, Uttarakhand, India

<sup>b</sup> Seismic Interpretation Laboratory-WIHG, India

### ARTICLE INFO

**Keywords:**

Carbonate reef  
Marine seismic  
Seismic attributes  
Structure  
Machine learning  
Offshore  
NW Australia

### ABSTRACT

A carbonate build-up or reef is a thick carbonate deposit consisting of mainly skeletal remains of organisms that can be large enough to develop a favourable topography. Delineation of such geologic features provides important input in understanding the basin's evolution and petroleum prospects. Here, we introduce a new attribute called the Reef Cube (RC) meta-attribute that has been computed by fusing several other seismic attributes that are characteristics of the reef through a supervised machine-learning algorithm. The neural learning resulted in a minimum nRMS error of 0.28 and 0.30 and a misclassification percentage of 1.13% and 1.06% for the train and test data sets. The Reef Cube meta-attribute has efficiently captured the anatomy of carbonate reef buried at ~450 m below the seafloor from high-resolution 3D seismic data in the NW shelf of Australia. The novel approach not only picks up the subsurface architecture of the carbonate reef accurately but also accelerates the process of interpretation with a much-reduced intervention of human analysts. This can be efficiently suited for delimiting any subsurface geologic feature from a large volume of surface seismic data.

### 1. Introduction

A carbonate reef is a thick carbonate deposit displaying an antecedent topography relative to the surrounding depositional surface (Heckel, 1974; Burgess et al., 2013). Carbonate reefs are attractive targets for hydrocarbon exploration in frontier and mature sedimentary basins (Burgess et al., 2013; Saqab and Bourget, 2015). Tectonic processes, eustasy, basinal physiography, and climatic conditions (Zampetti et al., 2004) control their evolution and geometry. They are potential stratigraphic traps and account for half of the global hydrocarbon reserves (Kusumastuti et al., 2002; Neuhaus et al., 2004; Ehrenberg et al., 2007; Ahr, 2011). The seismic reflection experiment is one of the best possible methods for delineating subsurface carbonate reefs. However, it might be challenging to interpret them accurately as they exhibit fundamental similarities to other geologic features, e.g., buried volcanoes, erosional remnants, or tilted fault blocks (Burgess et al., 2013; Niyazi et al., 2021).

The processing/modeling of seismic data has made substantial progress over the past decade, significantly improving subsurface images (Burgess et al., 2013; Kumar and Sain, 2018; Kumar et al., 2019; Kumar and Sain, 2020; Sain and Kumar, 2022). Human analysts or

interpreters primarily use seismic attributes to capture the structural geometry and disposition of subsurface features from the derived images. However, interpreters need help to derive accurate information about a specific geologic target. An individual seismic attribute is not uniquely responsive to a particular geologic body and thus cannot distinguish objects of different origins (Kumar and Sain, 2018; Kumar et al., 2019; Kumar and Sain, 2020; Sain and Kumar, 2022; Niyazi et al., 2022). Hence, the impact of an attribute's geological non-uniqueness and non-completeness keeps changing based on its usage and is entirely interpretation-dependent (Sain and Kumar, 2022).

Here we attempt to provide a unique solution to such a perplexing scenario by designing a new attribute, defined as the Reef Cube (RC) meta-attribute, using a fully connected multi-layer perceptron neural network following the supervised scheme of machine learning that allows a machine or intelligent system to learn and get equipped in solving a complex problem for prediction of the desired result. A set of computer-oriented programs are employed on a small portion of data (preferably 20%) during the learning process to accelerate the realistic interpretation of the entire volume of data without extensive human intervention (Kumar and Sain 2018, 2020; Kumar et al., 2019; Sain and Kumar 2022). Since the Browse Basin on the NW shelf off Australia has

\* Corresponding author. Wadia Institute of Himalayan Geology, 33 GMS Road, Uttarakhand, India.

E-mail addresses: [kumarchinmoy@gmail.com](mailto:kumarchinmoy@gmail.com) (P.C. Kumar), [kalachandsain7@gmail.com](mailto:kalachandsain7@gmail.com) (K. Sain).

developed a reef-rimmed carbonate platform during the Miocene period, we have looked into the high-quality 3D seismic data for the delimitation of the 3D subsurface architecture of carbonate reefs. First, we computed the seismic attributes that can characterize the carbonate reefs and then amalgamated them into a single hybrid attribute, termed the RC meta-attribute, using a machine learning algorithm. The presence of meta-attribute within the data volume, implying the existence of carbonate deposition, can now elucidate the anatomy of carbonate reef automatically from huge data volume with a much-reduced human intervention.

## 2. Tectonic structure of the browse basin

The Browse Basin is a 140,000 km<sup>2</sup> offshore extensional sedimentary basin in Australia's NW Shelf region (Fig. 1). The basin resembles a pond-like sedimentary depocentre (Rosleff-Sorensen et al., 2016), bounded by the Scott Plateau on the west and Leveque Shelf to the east. It embraces several half-graben structures that dip landwards and strike parallel to the margin (Struckmeyer et al., 1998). The primary depocenters of the basin are the Caswell and Barcoo sub-basins, which

contain a thick pile of Paleozoic, Mesozoic, and Cenozoic sedimentary successions (Fig. 1). Tectonically the Browse Basin evolved because of the Jurassic continental rifting between Greater India and Western Australia (Müller et al., 1998; Kaiko and Tait 2001; Langhi and Borel, 2007). The final phase of the rifting occurred in the Middle Jurassic and Early Cretaceous that generated a dominant SW-NE-oriented structural trend of the basin (Fig. 1b). During the Aptian, the tectonic activity ceased and the basin was covered with a thick sequence of passive-margin sediments (Struckmeyer et al., 1998).

The evolution of Browse basin initiated during the Late Carboniferous because of an extensional phase associated with the separation of Sibumasu from NW Australia (Struckmeyer et al., 1998; ConocoPhillips, 2012; Dixit and Mandal, 2020). This resulted into the formation of a series of extensional intra-cratonic half-graben structures in the basin. Initially fluvio-deltaic sediments infilled basin in the Carboniferous, then grading into marine shales and limestones in the Lower Permian. The basin then underwent a phase of thermal subsidence in the Late Permian continuing through to the Triassic (Struckmeyer et al., 1998; ConocoPhillips, 2012). The Permian to Middle Triassic post-rift sag phase resulted in deposition of shales, sands, carbonates of the Hyland bay Formation and marine shales of the Mt. Godwin formation. A period of increased tectonism commenced in the Late Triassic, with the initiation of the break-up of Australia from the Argoland. The Early to Middle Jurassic marked extensional event resulting in widespread, small scale faulting and collapse of the Triassic anticlines. Minor faulting occurred in the Late Jurassic to Early Cretaceous associated with Callovian break-up event along the NW margin of Australia. This event was followed by a period of relative tectonic quiescence in the Browse Basin. An overall transgressive cycle commenced in the Early cretaceous and peaked by Middle Turonian, with open marine conditions established throughout the basin. Basin infill in the Early Tertiary lead to shallow marine sedimentation across the Browse Basin.

As the Australian plate moved northward due to seafloor spreading in the Indian and Southern Oceans, the dominant sediment type on the NW shelf shifted from siliciclastic to carbonate during the Cenozoic era Struckmeyer et al., (1998); ConocoPhillips (2012); Dixit and Mandal (2020). The Early-Middle Miocene period witnessed the development of a typical reef-rimmed carbonate platform in the Browse Basin, which formed part of an unbroken reef belt extending along the NW shelf margin of Australia (Rosleff-Sorensen et al., 2012). Most of the present-day reefs in the basin and nearby areas grew on this extensive foundation of paleo-reefs and carbonate build-ups (Ryan et al., 2009).

## 3. Data and methods

This research uses a time-migrated 3D seismic cube of the Poseidon survey area in the Browse Basin, North-west shelf offshore Australia. The survey was operated by ConocoPhillips in 2010 (ConocoPhillips, 2012) and was acquired by CGG Veritas using the seismic vessel Geowave Voyager (ConocoPhillips, 2012). The survey covered a total area of 2828 km<sup>2</sup>. The survey's primary objective was to provide detailed subsurface coverage of potential exploration leads within the Cretaceous and Jurassic formations of the basin. The seismic data consist of 3436 inlines (range: 983–4419) and 5052 crosslines (range: 504–5556) and was acquired using a bin size of 18.75 m × 12.5 m (inline × crossline), with a 2 ms sampling interval and total recorded length of 6 s. The data was processed using conventional processing sequences, including noise attenuation, tidal static corrections, radon transform for residual linear noise attenuation, NMO corrections, velocity analysis, multiple attenuation, and frequency-dependent offset noise attenuation followed by Kirchhoff time migration. The survey region consists of four exploration wellbores: Poseidon 1, Poseidon 2, Kronos 1, and Torosa 1 (ConocoPhillips, 2012).

The methodology (Fig. 2), designed for this study, includes four (4) basic steps: (a) Structural enhancement of 3D seismic data; (b) Selection of seismic attributes suited to characterize carbonate reef; (c) Picking

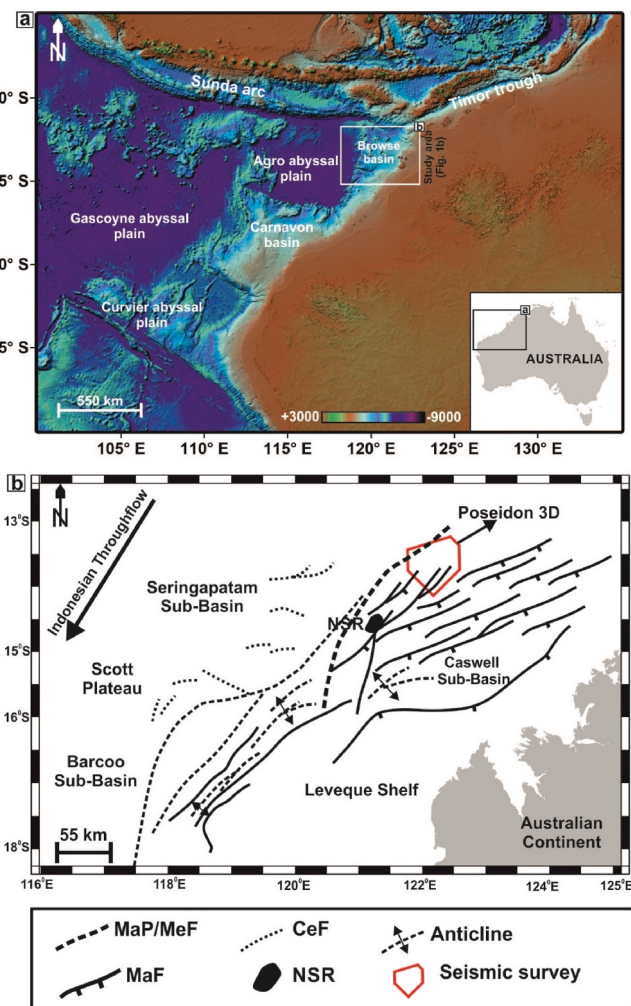


**Fig. 1.** (a) Browse Basin, located in the NW shelf of offshore Australia based on the Gridded Bathymetry Chart of the Oceans (GEBCO); (b) Geo-tectonic map of the Browse Basin showing different structural elements that chiefly strikes northeast. The basin is bounded by the Scott Plateau on the west and Leveque Shelf to the east. The Poseidon 3D seismic survey is shown in red rectangular polygon. MaP/MeF: Major Paleozoic/Mesozoic fault; MaF: Major Fault; CeF: Cenozoic Fault; NSR: North Scott Reef.

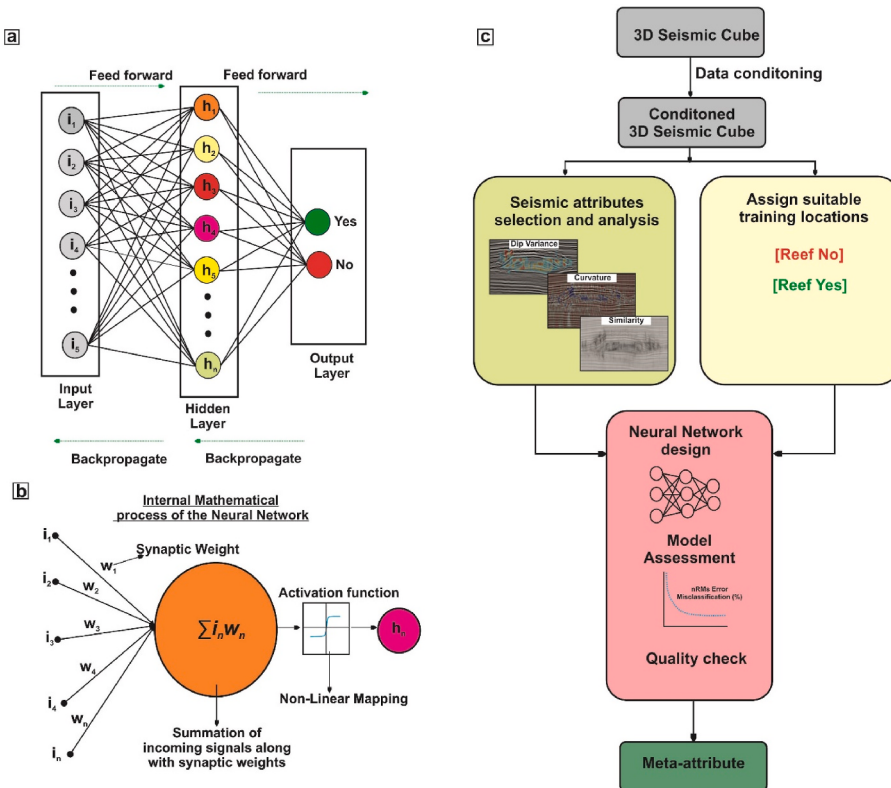


**Fig. 2.** (a, b) Structure and process of Neural Network used in the present research; (c) Proposed workflow for the computation of Reef Cube meta-attribute.

example locations, and (d) Neural Modelling. These steps are elaborated on in succeeding paragraphs.

### 3.1. Structural enhancement of 3D seismic data

Structural conditioning of seismic data maintains the lateral continuity of seismic events and provides enhanced subsurface structural images (Kumar and Sain, 2018; Sain and Kumar, 2022). We have enhanced the 3D seismic cube through a classical dip-steering technique, resulting in a steering cube (or a dip-azimuth volume) (Tingdahl, 1999, 2003; Kumar and Mandal, 2017). The cube contains seismic dip and azimuth information at every sample position. A 3D Fourier Transform-based dip algorithm proposed by Tingdahl (2003) is used to compute the steering cube. The algorithm produces a stable dip-azimuth steering volume. The dip-azimuth is calculated at every sample by transforming a sub-cube of  $3 \times 3 \times 3$  samples to the 3D Fourier domain. The maximum dip is estimated with the help of a third-order polynomial curve fitting (Tingdahl, 2003) to the sub-cube around the sample of the highest energy in the Fourier domain. Then a search for the local maxima is done, and the corresponding dip-azimuth to the local maxima is set as the output. The operation is performed throughout the seismic volume to generate the dip-azimuth volume, called the 'Detailed Steering Cube' (DSC), and stores detailed structural information. Use of coarser median filtering to the DSC by a filtering step out, i.e.,  $\text{inl: } \text{xrl: sample } 5 \times 5 \times 5$ , results in a steering cube, which is now called the 'Background Steering Cube' (BSC). It contains the overall dip trends of seismic reflectors and outlines the background structural information. For the present study, the DSC is deemed the best, as the research aims to capture the detailed structural architecture of the geological target.

The DSC is taken as an input for data enhancement through structural filtering (Kumar and Sain, 2018). Structural filtering is performed using a structure-oriented filter (SOF). The key objective of using the SOF is to differentiate between the dip-azimuth of seismic reflectors and overlying noises (Kumar and Sain, 2018; Sain and Kumar, 2022). This

not only removes the noise bursts but also enhances the lateral continuity of seismic events (Höcker and Fehmers, 2002) and ultimately provides smooth and improved images of geological structures (Kumar and Mandal, 2017; Kumar and Sain, 2018; Sain and Kumar, 2022). This is carried out using a dip-steered median filter (DSMF), which employs median statistics over amplitudes ensuing the dip of seismic reflectors (Kumar and Sain, 2018; Sain and Kumar, 2022). A filtering step-out of  $3 \times 3$  is used to execute the filtering operation. This resulted in a filtered seismic cube (also known as the DSMF cube), which, after a detailed quality check, is used to extract seismic attributes, select training/testing locations, and design the neural model.

### 3.2. Seismic attributes and their selection

Seismic attributes efficiently interpret the structural geometry and configuration of geologic features from 3D seismic data volume (Kumar and Sain, 2018; Sain and Kumar, 2022). To begin the selection of seismic attributes, it is crucial to understand the geological characteristics of carbonate platforms. A carbonate build-up demonstrates an antecedent topography and is associated with high-amplitude capping reflections (Zampetti et al., 2004; Burgess et al., 2013). Internally, the reflections vary from moderate to high amplitudes and are stacked parallel one upon the other (Zampetti et al., 2004; Burgess et al., 2013). Their marginal ends are typically associated with localized thickening, and their depositional wings exhibit variable dips. Faults at either end of their flanks make reflections weakly correlated. Above the build-ups, very often, there occurs any absence of equivalent overburden structures. Moreover, sediments onlap along their flanks, forming wedge-like structures. Being governed by these characteristics, in seismic data, the carbonate build-ups are associated with high energy capping reflections, possess variable dips along the flanks, and demonstrate a convex-up geometry. Moreover, they exhibit discontinuous geometry along the dipping edges of the flanks. Hence, a suitable set of seismic attributes, such as similarity, dip angle variance (DAV), energy, curvature, and

reference time (Table 1), have been chosen to arrest these geophysical signatures. The readers can refer to other works of authors (Kumar and Sain, 2018, 2020; Kumar et al., 2019; Sain and Kumar, 2022) for the definitions and mathematical equations about these attributes.

### 3.3. Example locations for training/testing

The labeled locations are marked arbitrarily along a few xlines and inlines. The Reef-yes and Reef-no locations are designated following the seismic signatures and geologic properties described in the previous paragraph. The Reef-yes locations are assigned binary number 1, and Reef-no locations are allocated binary number 0 according to the classification rule of binary numbers. Ambiguous areas where there is no hint of the presence of the target or the areas that are devoid of the target are avoided. About 870 Reef-yes and 880 Reef-no locations are labeled for training and testing. The binary data (0, 1) and seismic attributes at the marked locations are fed into the neural model for training and testing. This entire process is summarized in the following steps.

- In the first step, we randomly examined the seismic lines for the presence of carbonate build-ups.
- In the second step, we further investigated the seismic characteristics of the target over these lines with the help of attribute responses.
- Combining the first and second steps, we selected appropriate locations that should be assigned for the network to learn.
- Neural training is then executed over these seismic lines to compute the meta-attribute.
- Once satisfied with the performance of the neural model, the network is made to scan over the entire seismic cube to generate the hybrid attribute, called the Reef Cube (RC) meta-attribute, which is then used to decipher the structural geometry of the buried carbonate reef.

### 3.4. Neural Modelling

We have designed a fully connected multi-layer perceptron (MLP) network to compute the RC meta-attribute from a suitable suite of seismic attributes to arrest the structural configuration of carbonate build-ups. The MLP consists of three distinct layers: the input, the hidden, and the output layers, which contain 5, 4, and 2 neurons, respectively. The seismic attributes and binary numbers at the picked/labeled locations are fed into the input layer. Neurons receive these data in the hidden layer, where they are grouped and rescaled using a sigmoidal function. This activation function splits the output into binary numbers, i.e., 0s and 1s, where 0 refers to the minimum probability of the carbonate reef and 1 signifies the maximum likelihood. Only 20% of the

**Table 1**  
Geometrical and seismic characteristics of carbonate reef.

Name of the Target	Geometry	Seismic Characteristics	Suitable Seismic attributes
Carbonate Reef	Positive antecedent topography	High amplitude capping reflections	Energy
	Localized Thickening	High dips at the marginal ends of the structure	Dip Variance
	Depositional wings (or on-lap)	Positive topography leading to convex-up structure Discontinuity along flank edges	Curvature (most positive) Similarity/ Coherency
	Margin related faulting	Discontinuous reflections	Similarity/ Coherency
	Absence of any equivalent overburden structure	Continuous and parallel reflections	–

data are randomly picked up for training and testing. Again, 70% of the picked data are used in training to predict any value between 0 and 1 using a feed-forward process (Poulton, 2001; Kumar and Sain, 2018). The network parameters (learning rate, momentum, and, most importantly, synaptic weights) are adjusted through successive iterations using the backpropagation procedure (Rosenblatt, 1962; Rumelhart et al., 1995) to reduce the differences between predicted and train responses (0,1). In this research, the learning rate and momentum are optimally set to 0.01 and 0.25, respectively, through several trials. Because the process also predicts at the remaining 30% of locations (test data), the difference between the expected response and the test data (0, 1) is calculated simultaneously to determine whether the network is performing appropriately by observing the nature of the difference curve, i.e., the steadily declining trend of difference with iterations (Kumar and Sain, 2018). Neural training through successive iterations is continued until there is a minimum normalized root-mean-square (nRMS) error and a minimum misclassification percentage between prediction and train/test data, resulting in a probability output at all selected locations. The network's performance is validated visually by co-rendering the predicted meta-attribute over other seismic lines that were not considered in training. Once this validation is complete, the network runs over the entire seismic cube, automating and speeding up the interpretation process. We must state that the probability output with more than 0.75 thresholds highlights the RC meta-attribute, which delimits the anatomy of the carbonate build-up in the entire three-dimensional space.

## 4. Results and interpretation

The Poseidon 3D seismic volume is contaminated with noisy reflections that mask the carbonate build-ups and pose disturbances for interpretation (Fig. 3a–b). Structural data conditioning improves visualization by removing noise bursts and making reflections laterally continuous (Fig. 3c–d). The build-up possesses an antecedent topography with high amplitude or energy-capping reflections (Fig. 4a). The platform of the build-up is associated with high energy. On the other hand, the internally layered geometry is a reduction in energy content (Fig. 4a). The flanks are associated with variable dips. In contrast, reflections are weakly correlated along the edges demonstrating low similarity (Fig. 4b–c). The overall anticlinal geometry of the build-up is enhanced by the positive curvature attribute (Fig. 4d). Hence, several attributes improve the interpretation by capturing the structural responses of the carbonate build-up or reef from the data.

In this research, the neural operation (Fig. 5a–c) yielded a minimum normalized root-mean-square (RMS) error (Fig. 5d) and minimum misclassification percentage (Fig. 5e) for both the train and test data sets. It is observed that the nRMS of 0.28 and 0.30 and minimum misclassification of 1.13% and 1.06% are achieved after 25 iterations for the train and test data sets, respectively. The relative contribution of the individual seismic attributes while training the system is given in Table 2. The reference time offers the maximum assistance to the neural training, followed by the DAV, energy, curvature, and similarity attributes. At each sample point of the 3D seismic volume, the neural network predicted values lying between 0 and 1. The values closer to 0 represent the minimum likelihood of carbonate build-up, and those closer to 1 elucidates the maximum possibility of carbonate build-up (Fig. 6). The maximum probability is interpreted using an optimal color scale (in Fig. 6 the meta-attribute is displayed using turquoise-sky blue-dull green-white-deep yellow-red color variations). The values of more than the 0.75 thresholds are considered as the Reef-Cube (RC) meta-attribute (Fig. 6).

The carbonate build-ups in the study area are associated with a positive topography with high amplitude capping reflections (Fig. 6a, c, and e). Their marginal ends are onlaped by a thick sediment wedge. Internally, reflections are stacked in parallel and are associated with moderate to high amplitude reflections. Such a stacking pattern

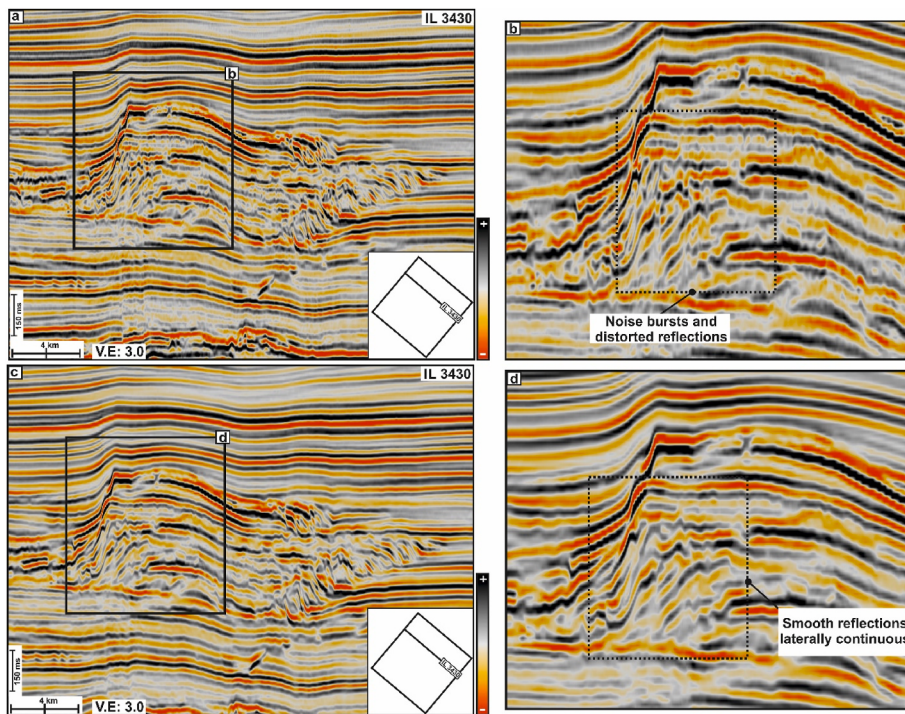


**Fig. 3.** (a) Original time migrated seismic section for IL 3430 from the Poseidon 3D survey; (b) zoomed view of the carbonate-build-up zone marked by black rectangle in (a). Internal reflections within the carbonate is noisy and are associated with amplitude bursts; (c) Dip Steered Median Filtered (DSMF) time migrated seismic section for the same line IL 3430; (d) zoomed view of carbonate build-up zone marked by black rectangle in (c) showing enhanced seismic reflections free from amplitude bursts within the carbonate build-up.

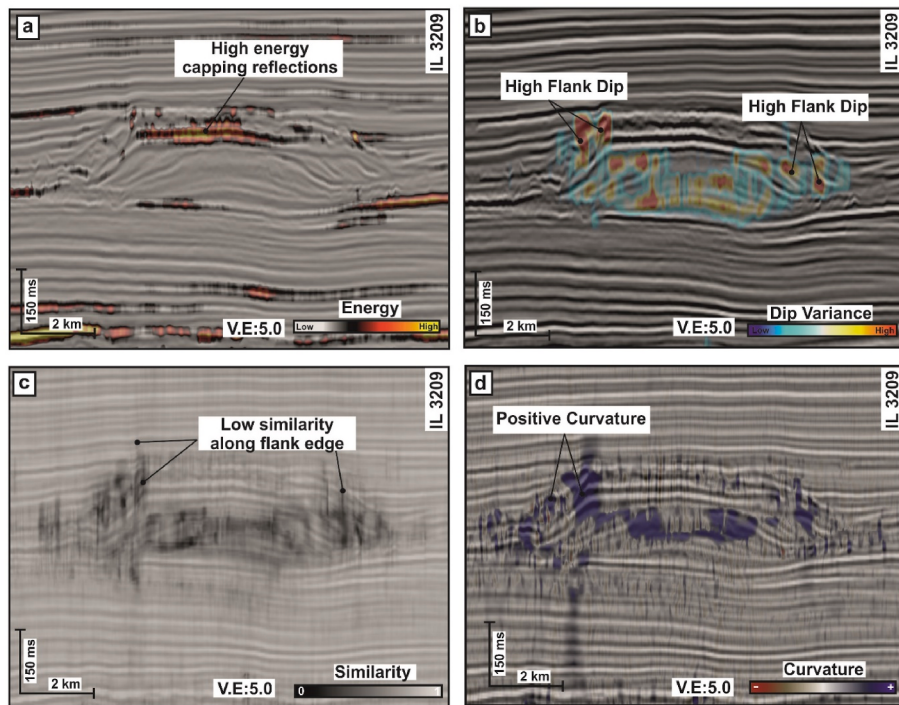


**Fig. 4.** Selected suitable seismic attributes e.g., (a) energy, (b) dip angle variance, (c) similarity and (d) curvature (most positive) attribute demonstrating seismic responses of carbonate build-ups, displayed by co-rendering with the seismic section for line IL 3209.

indicates different growth stages of the build-up. The RC meta-attributes have efficiently captured these phenomena by isolating the build-ups from the surrounding sedimentary successions (Fig. 6b, d, f, and g). The co-rendered view of the amplitude cube and RC meta-attribute have revealed detailed structural geometry of the carbonate build-ups or reef observed over the time map sliced at  $t = 1168$  ms and  $t = 1244$  ms (Fig. 7a–f), respectively. The carbonate reefs consist of several symmetrical rings stacked upon one another, showing an elbow geometry.

Their crest contains several small reef patches with circular geometry (Fig. 7b–d).

To validate the RC meta-attribute's outcome, we compared the structurally filtered seismic section (Fig. 6e) with the machine-generated RC meta-attribute co-rendered with the same section (Fig. 6f and g), which was not included while training the system. The visual inspection shows that the predicted RC meta-attribute has captured the structural configuration of the carbonate build-up from the

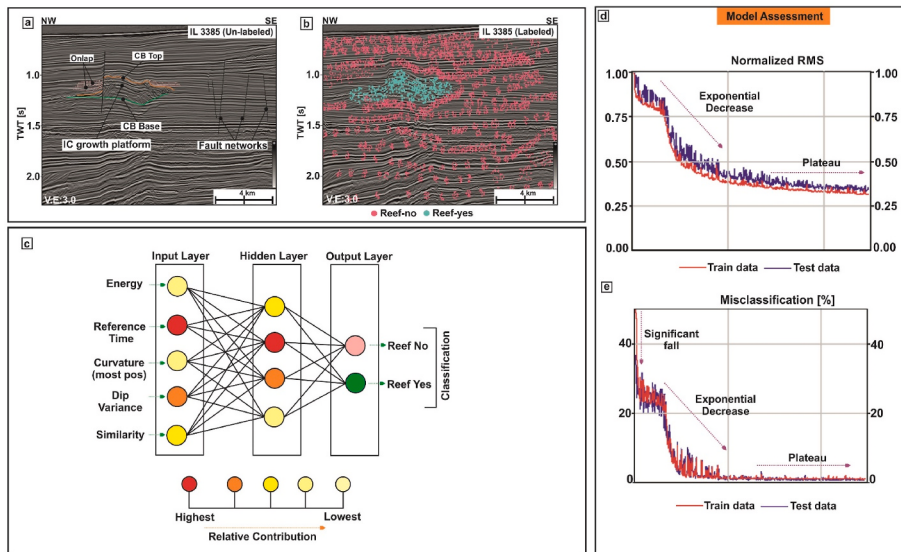


**Table 2**  
Relative contribution of seismic attributes during training the Neural Model.

Seismic Attributes	Weights
Energy	72
Reference Time	98
Similarity	55
Dip Variance	82
Curvature(Most Positive)	57

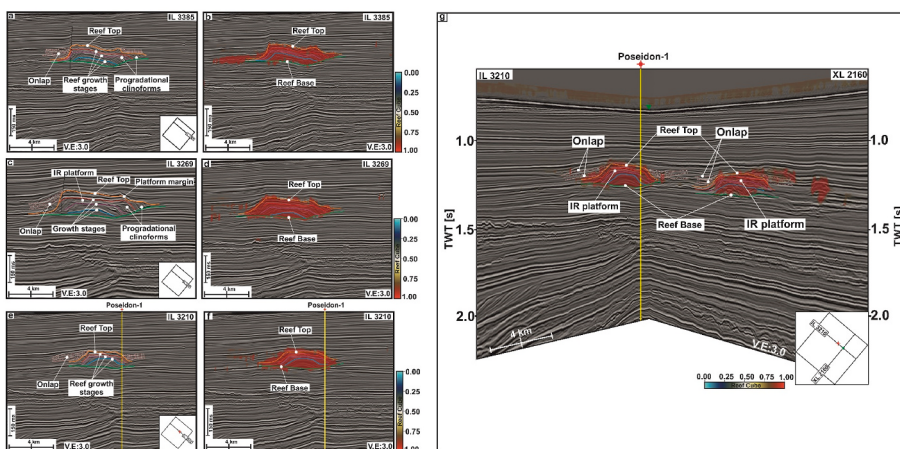
seismic cube. Based on the threshold value of 0.75 for the RC meta-attribute, we could generate the 3D structural anatomy of the buried carbonate build-ups (Fig. 6). The elbow geometry, circular geometry of small reef patches at the crest, and stepped growth platforms are illuminated automatically. The neural model resembles a "deep-seated cake" structure (Fig. 8) buried ~450 m below the seafloor in the Browse Basin off Australia.

## 5. Discussion

### 5.1. Reef Cube as a new interpretation tool for interpreting buried carbonate reefs on seismic reflection data

#### 5.1.1. Effect of structural conditioning of seismic data

Seismic data, when contaminated by coherent or random noise, the S/N ratio decreases and lowers the accuracy of static and dynamic corrections during the processing stage. This finally degrades the quality of the processed seismic cross-sections (Liu et al., 2006; Onajite, 2014). As a result, interpreters struggle to interpret the buried carbonate reefs and their internal anatomy precisely. Advanced data conditioning approaches help to overcome such problems. The initial phase of this research's workflow aimed at improving the seismic responses of the buried carbonate reefs from reflection seismic data. The original time-migrated 3D seismic data from the Poseidon seismic survey show that the carbonate reef is associated with distorted seismic signals and noisy events (Fig. 3a–b). To circumvent such problems, we have applied a structure-oriented filter called the DSMF to remove the noises that surround and mask the carbonate reef. The filter uses a pre-processed steering cube and a median statistic (i.e., computation of median between the sample values) over seismic amplitudes following the seismic



IR: Internal Reef.

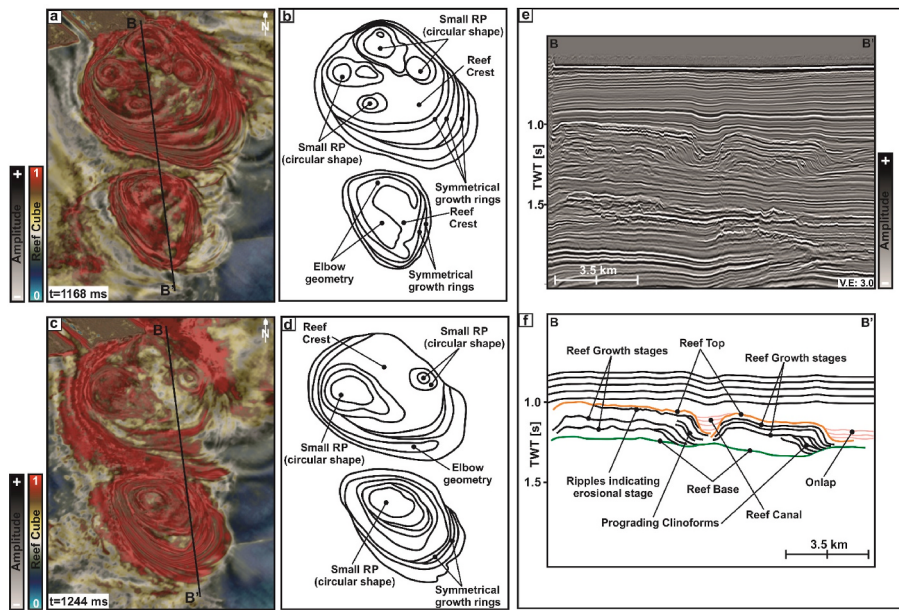


**Fig. 7.** (a, c) Time maps, sliced at  $t = 1168$  ms and  $t = 1244$  ms respectively, by co-rendering the seismic amplitude cube with the RC meta-attribute; (b, d) Line drawings corresponding to the same time maps showing the structural elements of the carbonate build-up; (e, f) Random seismic line BB' and the corresponding interpretation. RP: Reef Patch.

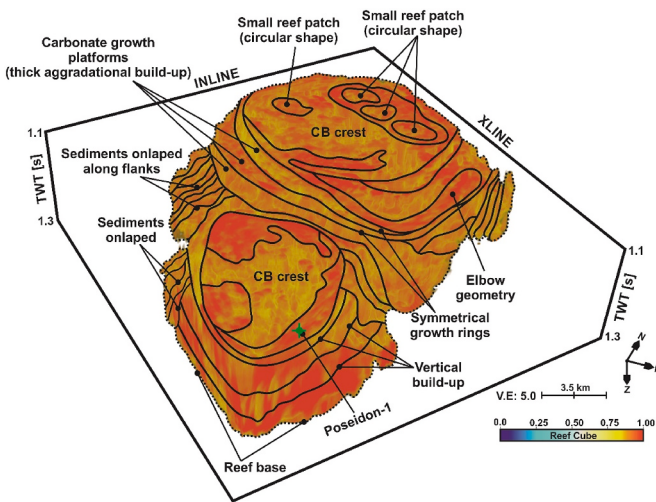


**Fig. 8.** 3D anatomy of the carbonate reef or build-up, as elucidated by the RC meta-attribute. The build-ups demonstrate a “deep seated cake” structural configuration. A pastel color scale is used to display the RC meta-attribute. The small reef patches (dark red color) have high probability of being identified as reef and CB crest and growth platforms (yellow to light red) have the low probability of being a reef. CB: Carbonate Build-up.

dips (Sain and Kumar, 2022). The filter effect is tested through different step-outs (e.g.,  $3 \times 3$ ;  $5 \times 5$ ;  $7 \times 7$ ). Over-smoothing of the amplitude content is avoided. Thus, applying a mild median filtering step-out (i.e.,  $3 \times 3$ ) to the data volume makes the amplitude content throughout the reef complex (both at the top and internally) laterally continuous, random noise gets suppressed, and the S/N ratio is enhanced. This, in turn, improves the visibility of the carbonate reef (associated with high amplitude content) from the surrounding environment in the conditioned seismic volume (see Fig. 3c-d and 6). The seismic conditioning not only preserves the structural architecture of the carbonate reef but also improves the signal quality (S/N) in and around the reef complex.

### 5.1.2. Manual interpretation versus neural network analysis

Manual interpretation, including auto-picking approaches, needs a careful recognition of carbonate reef complexes from seismic data (Burgess et al., 2013; Saqab and Bourget, 2015; Van Tuyl et al., 2019). However, it becomes successful only when interpreters can effectively distinguish these targets based on their geologic and seismic characteristics (see Table 1) from the host-rock strata and geophysical artifacts. Analysis of individual seismic attributes have been efficient in such case, but their success depends mainly on adequate parameter settings to capture the maximum geological responses from the data (Chopra and Marfurt, 2007; Barnes, 2016; Sain and Kumar, 2022). Furthermore, the downside of using a single attribute for such interpretation is that a seismic attribute on its own hardly ever responds to a geological target of interest and thus brings out a mixed set of geological responses (Meldahl et al., 2002; Tingdahl, 2003; De Groot et al., 2004; Kumar and Sain, 2018; Sain and Kumar, 2022; Niyazi et al., 2022). In the present study, we aim to bring out a realistic interpretation of reef complexes through a neural network approach. These targets are interpreted based on the interpreter’s judgment. Based on the geological characteristics of the target (see Table 1) and the interpreter’s geological knowledge, locations that mark the presence of carbonate reefs (i.e., the maximum probability) and locations that are devoid of carbonate reefs (i.e., the least probability) are selected (Fig. 5a-b). This judgment is then counterchecked with the responses revealed by multiple seismic attributes (see Table 1). Finally, the judgment and the responses are linked through a fully connected MLP network to minimize the error so that an optimal output is obtained (Fig. 5d-e). This, in turn, generates a meta-attribute that brings out enhanced images of the target (as per the present research, it is the carbonate reef complex). The Reef Cube meta-attribute in this study illuminated the “deep-seated cake” architecture and the internal anatomy of the buried carbonate reef from seismic reflection data (Fig. 8).

### 5.2. Limitations

The RC meta-attribute is a neural network approach that aims to illuminate the structural architecture of buried reef complexes from 3D seismic data by exploiting the generalization capability of artificial neural networks (ANNs). The downside of this approach relates to the

use of noisy or poor-quality data as input for the computation of the meta-attribute. Using such data may result in feeding inaccurate example locations to the network. As a result, the learning capability of the neural network decreases, and thus the generalization efficiency of the NN fails, making the network to output artifacts. This thus impedes the interpretation. In such instances, the computed meta-attribute may scuffle to deliver a successful interpretation of reef complexes from the data volume.

## 6. Conclusions

This research shows that interpreting subsurface geologic features through an amalgamation of suitable seismic attributes, guided by an interpreter's acquaintances, results in a hybrid attribute or the so-called meta-attribute (Figs. 4–6). Though an individual attribute captures the seismic response of subsurface geologic structures from the data, a suitable combination improves the images of subsurface targets and reduces interpretation uncertainties. This research's newly designed RC meta-attribute has efficiently isolated the structural anatomy of buried carbonate reefs or build-ups from the 3D seismic volume (Figs. 6–8). The carbonate build-up delimited through the computation of the RC meta-attribute, resembles a "deep-seated cake" consisting of several vertically stacked platforms, giving rise to an antecedent topography (Fig. 8). Seismic interpreters can employ this neural-based approach to delimit the structural anatomy of carbonate reservoirs from 3D seismic data acquired over sedimentary basins worldwide. Thus, the meta-attribute sets an example for advanced interpretation of seismic data over an individual attribute analysis.

## Data availability

The data used in this research is publicly available and can be found online. The seismic data and reports are available from Geoscience Australia (<http://www.ga.gov.au/>). Conoco Philips shared this data in the public domain through the Google Drive link (<https://drive.google.com/drive/folders/0B7brcf-eGK8CRUhfRW9rSG91bW8?resourcekey=0-NsLk7JL-IDDxUKPVp0dZrw>).

## Appendix

### A. Normalized Root Mean Square Error (nRMS)

The nRMS error is computed from the RMS error (Eq. A.1) between the targeted ( $t_i$ ) and computed ( $c_i$ ) values for  $i$  ranging from 1 to  $n$ , which is given as (Eq. A.2) (Kumar and Sain, 2018):

$$RMS = \sqrt{\frac{1}{n} \sum_{i=1}^n (t_i - c_i)^2} \quad (\text{A.1})$$

$$\text{normalized RMS} = RMS \left/ \sqrt{\frac{1}{n} \sum_{i=1}^n (t_i - \text{mean})^2} \right. \quad (\text{A.2})$$

where the mean is given as in Eq. A.3:

$$\text{mean} = \frac{1}{n} \sum_{i=1}^n t_i \quad (\text{A.3})$$

The nRMS error curve demonstrates the overall error on the train and test data sets, with a scale ranging from 0 to 1, where 0 corresponds to no error, and 1 corresponds to the highest error. It has been demonstrated that the lower the nRMS, the better the neural outcome is (Kumar and Sain, 2018, 2020; Kumar et al., 2019; Sain and Kumar, 2022). The other benefit is that error performance can be observed from a single graph display.

### B. Misclassification percentage (%)

The misclassification percentage is a quality control parameter to understand the wrong predictions made during the classification. To have control over this accuracy, creating a truly representative distribution of the observations for each class (i.e., target and non-target zones) is good enough. The

## Author contributions

**P.C.K. (the first author):** Conceptualisation, Data curation and interpretation, Methodology, Investigation, Visualization, Project administration, Writing, Figures-drafting, Review, and Editing, OpendTect™ Software Resources. **K.S (the second author):** Review and Proofread, Software Resources.

## Funding

There is no funding associated with this work.

## Declaration of conflict interest

The authors declare that they have no known competing financial interests or personal relationships that could have appeared to influence the work reported in this paper.

## Acknowledgements

Director, WIHG, Dehradun, is grateful for permission to publish this work. The authors acknowledge GeoScience Australia for making the seismic data and petroleum reports publicly available under this research's Creative Commons Attribution 3.0 Australia (CC BY 3.0 AU) license. dGB Earth Sciences is duly acknowledged for providing software support (OpendTect™ v5.0 & v6.0) for this work. Halliburton™ is thanked for providing the DSG interpretation suite. Geosoftware™ is thanked for providing academic licence of Hampson Russell 13.0 and Jason 12.0 for this research. The authors are thankful to the anonymous reviewers, and the Editor-in-Chief Gabriele Morra for the comments and valuable suggestions on earlier version of this manuscript. GECO Compilation Group (2019) is thanked for making gridded bathymetry files freely available for academic research. KS acknowledges DST-SERB for according him with JC Bose National Fellowship. This is a Wadia contribution no. WIHG/0274.

classification percentage (Eq. B.1) is the ratio of correct predictions to the total number of predictions.

$$\text{Classification (\%)} = \frac{\text{Number of correct predictions}}{\text{Total number of predictions}} \times 100 \quad (\text{B.1})$$

The misclassification percentage (Eq. B.2) is defined as the ratio of wrong predictions to the total number of predictions.

$$\text{Misclassification (\%)} = \frac{\text{Number of wrong predictions}}{\text{Total number of predictions}} \times 100 \quad (\text{B.2})$$

## References

- Ahr, W.M., 2011. Geology of Carbonate Reservoirs: the Identification, Description and Characterization of Hydrocarbon Reservoirs in Carbonate Rocks. John Wiley & Sons.
- Barnes, A.E., 2016. Handbook of Post-stack Seismic Attributes. SEG, Tulsa.
- Burgess, P.M., Winefield, P., Minzoni, M., Elders, C., 2013. Methods for identification of isolated carbonate buildups from seismic reflection data/Identification of Isolated Carbonate Buildups from Seismic Reflection Data. AAPG Bull. 97 (7), 1071–1098.
- Chopra, S., Marfurt, K.J., 2007. Seismic Attributes for Prospect Identification and Reservoir Characterization. SEG, Tulsa.
- ConocoPhillips, 2012. Poseidon 3D Marine Surface Seismic Survey Interpretation Report (unpublished). <https://drive.google.com/drive/folders/0B7brcf-eGK8Cbk9ueH> A0QUU4Zjg.
- De Groot, P., Ligtenberg, H., Oldenziel, T., Connolly, D., Meldahl, P., 2004. Examples of multi-attribute, neural network-based seismic object detection. Geological Society 29 (1), 335–338. London, Memoirs.
- Dixit, A., Mandal, A., 2020. Detection of gas chimney and its linkage with deep-seated reservoir in Poseidon, NW shelf, Australia from 3D seismic data using multi-attribute analysis and artificial neural network approach. J. Nat. Gas Sci. Eng. 83, 103586.
- EHrenberg, S.N., Nadeau, P.H., Aqrabi, A.A.M., 2007. A comparison of Khuff and Arab reservoir potential throughout the Middle East. AAPG Bull. 91 (3), 275–286.
- Heckel, P.H., 1974. Carbonate Build-Ups in the Geologic Record: a Review. <https://doi.org/10.2110/pec.74.18.0090>.
- Höcker, C., Fehmers, G., 2002. Fast structural interpretation with structure-oriented filtering. Lead. Edge 21 (3), 238–243.
- Kaiko, A.R., Tait, A.M., 2001. Post-rift tectonic subsidence and paleo-water depth in the northern Carnarvon basin, western Australia. APPEA J 41, 367–380.
- Kumar, P.C., Mandal, A., 2017. Enhancement of fault interpretation using multi-attribute analysis and artificial neural network (ANN) approach: a case study from Taranaki Basin, New Zealand. Explor. Geophys. 49 (3), 409–424.
- Kumar, P.C., Sain, K., 2018. Attribute amalgamation-aiding interpretation of faults from seismic data: an example from Waitara 3D prospect in Taranaki basin off New Zealand. J. Appl. Geophys. 159, 52–68, 2018.
- Kumar, P.C., Sain, K., 2020. A machine learning tool for interpretation of Mass Transport Deposits from seismic data. Nature Scientific Reports 10 (1), 1–10.
- Kumar, P.C., Omosanya, K.O., Alves, T., Sain, K., 2019. A neural network approach for elucidating fluid leakage along hard-linked normal faults. Mar. Petrol. Geol. 110, 518–538.
- Kusumastuti, A., Van Rensbergen, P.V., Warren, J.K., 2002. Seismic sequence analysis and reservoir potential of drowned Miocene carbonate platforms in the Madura Strait, East Java, Indonesia. AAPG Bull. 86 (2), 213–232.
- Langhi, L., Borel, G.D., 2007. Reverse structures in accommodation zone and early compartmentalization of extension system, Laminaria High (NW shelf, Australia). Mar. Petrol. Geol. 25, 791–803, 2007.
- Liu, C., Liu, Y., Yang, B., Wang, D., Sun, J., 2006. A 2D multistage median filter to reduce random seismic noise. Geophysics 71 (5), V105–V110.
- Meldahl, P., Najjar, N., Oldenziel-Dijkstra, T., Ligtenberg, H., 2002. Semi-automated detection of 4D anomalies. In: In64th EAGE Conference & Exhibition. EAGE Publications BV cp-5.
- Müller, R.D., Mihut, D., Baldwin, S., Purcell, P.G., Purcell, R.R., 1998. A new kinematic model for the formation and evolution of the west and northwest Australian margin. The sedimentary basins of Western Australia 2, 55–72.
- Neuhaus, D., Borgoman, J., Jauffred, J.C., Mercadier, C., Olotu, S., Grtsch, J., 2004. Quantitative Seismic Reservoir Characterization of an Oligocene Miocene Carbonate Build-Up: Malampaya Field, Philippines, vol. 81. AAPG Memoir, pp. 169–183.
- Niyazi, Y., Eruteya, O.E., Warne, M., Ierodiaconou, D., 2021. Discovery of large-scale buried volcanoes within the Cenozoic succession of the Prawn Platform, offshore Otway Basin, southeastern Australia. Mar. Petrol. Geol. 123, 104747.
- Niyazi, Y., Warne, M., Ierodiaconou, D., 2022. Machine learning delineation of buried igneous features from the offshore Otway Basin in southeast Australia. Interpretation 10 (3), SE101–SE118.
- Onajite, E., 2014. Understanding noise in seismic record. In: Seismic Data Analysis Techniques in Hydrocarbon Exploration. Elsevier, Amsterdam, pp. 63–68.
- Poulton, M.M., 2001. Computational Neural Networks for Geophysical Data Processing. Elsevier, London.
- Rosenblatt, F., 1962. Principles of Neurodynamics. Perceptrons and the Theory of Brain Mechanisms (No. VG-1196-G-8). Cornell Aeronautical Lab Inc Buffalo NY.
- Rosleff-Soerensen, B., Reuning, L., Back, S., Kukla, P., 2012. Seismic geomorphology and growth architecture of a Miocene barrier reef, Browse Basin, NW-Australia. Mar. Petrol. Geol. 29 (1), 233–25.
- Rosleff-Soerensen, B., Reuning, L., Back, S., Kukla, P.A., 2016. The response of a basin-scale Miocene barrier reef system to long-term, strong subsidence on a passive continental margin, Barcoo Sub-basin, Australian North West Shelf. Basin Res. 28 (1), 103–123.
- Rumelhart, D.E., Durbin, R., Golden, R., Chauvin, Y., 1995. Backpropagation: the basic theory. Backpropagation: theory, architectures and applications 1–34.
- Ryan, G., Bernardel, G., Kennard, J., Jones, A.T., Logan, G., Rollet, N., 2009. A pre-cursor extensive Miocene reef system to the Rowley Shoals reefs, Western Australia: evidence for structural control of reef growth or natural hydrocarbon seepage? The APPEA Journal 49 (1), 337–364.
- Sain, K., Kumar, P.C., 2022. Meta-attributes and Artificial Networking: A New Tool in Seismic Interpretation. AGU-John Wiley & Sons.
- Saqab, M.M., Bourget, J., 2015. Controls on the distribution and growth of isolated carbonate build-ups in the Timor Sea (NW Australia) during the Quaternary. Mar. Petrol. Geol. 62, 123–143.
- Struckmeyer, H.I.M., Blevin, J.E., Sayers, J., Totterdell, J.M., Baxter, K., Cathro, D.L., 1998. Structural evolution of the Browse Basin, North west shelf: new concepts from deep-seismic data. In: Purcell, P.G., Purcell, R.R. (Eds.), The Sedimentary Basins of Western Australia 2: Proceedings of the Petroleum Exploration Society of Australia Symposium, vol. 1998, pp. 345–367 (Perth, WA).
- Tingdahl, K.M., 1999. Improving seismic detectability using intrinsic directionality: technical report, B194. In: Earth Sciences Centre. Goteborg University.
- Tingdahl, K.M., 2003. Improving seismic chimney detection using directional attributes. In: Developments in petroleum scienceElsevier 51, 157–173.
- Van Tuyl, J., Alves, T., Cherns, L., Antonatos, G., Burgess, P., Masiero, I., 2019. Geomorphological evidence of carbonate build-up demise on equatorial margins: a case study from offshore northwest Australia. Mar. Petrol. Geol. 104, 125–149.
- Zampetti, V., Schlager, W., van Konijnenburg, J.H., Everts, A.J., 2004. Architecture and growth history of a Miocene carbonate platform from 3D seismic reflection data; Luconia province, offshore Sarawak, Malaysia. Mar. Petrol. Geol. 21 (5), 517–534.